Paper ID# B020

Metal Decorated Multi-Walled Carbon Nanotube/Polyimide Composites with High Dielectric Constants and Low Loss Factors

Sayata Ghose[1], Kent A. Watson[1], Holly A. Elliott[2], Keun J. Sun[1], Kenneth L. Dudley[2], Joseph G. Smith Jr.[2] and John W. Connell[2]

[1]National Institute of Aerospace, Hampton, VA 23666-6147
[2]NASA Langley Research Center, Hampton, VA 23681-2199

Abstract

The measurement of observable electromagnetic phenomena in materials and their derived intrinsic electrical material properties are of prime importance in the discovery and development of material systems for electronic and aerospace applications. Nanocomposite materials comprised of metal decorated multi-walled carbon nanotubes (MWCNTs) were prepared by a facile method and characterized. Metal particles such as silver(Ag), platinum(Pt) and palladium(Pd) with diameters ranging from less than 5 to over 50 nanometers were distributed randomly on the MWCNTs. The present study is focused on silver decorated MWCNTs dispersed in a polyimide matrix. The Ag-containing MWCNTs were melt mixed into Ultem™ and the mixture extruded as ribbons. The extruded ribbons exhibited a moderate to high degree of MWCNT alignment as determined by HRSEM. These ribbons were then fabricated into test specimens while maintaining MWCNT alignment and subsequently characterized for electrical and electromagnetic properties at 8-12 GHz. The results of the electromagnetic characterization showed that certain sample configurations exhibited a decoupling of the permittivity (ε') and loss factor (ε") indicating that these properties could be tailored within certain limits. The decoupling and independent control of these fundamental electrical material parameters offers a new class of materials with potential applications in electronics, microwave engineering and optics.

Keywords: Dielectric materials, carbon nanotubes, permittivity, loss factor, electrical properties, high-k materials, artificial crystalline dielectrics

Corresponding author: Sayata Ghose, Sayata.ghose-1@nasa.gov, 1-757-864-2094

1. INTRODUCTION

Tunable and tailorable dielectric materials are critical technologies necessary to meet and advance science and engineering goals important in many commercial, industry, and government technology development programs. With growing technology and application possibilities there has been considerable research and progress in materials development. Unfortunately tunable and tailorable materials to date have been limited in bandwidth and suffer unacceptably high losses.

An ideal semiconducting material should have a relatively high electrical permittivity, good thermodynamic stability, high interface quality, and optimal process compatibility. Of these characteristics, electrical permittivity is of particular importance in the design of capacitors and other electronic components and devices. The electrical permittivity of any substance is a property that is intrinsic to the material itself, and is independent of the thickness of the material. In general terms, electrical permittivity describes the manner in which a particular dielectric material affects an incident electric field [1]. The electrical permittivity of a given dielectric material is often expressed via the dielectric's complex electrical permittivity (ε), a term containing both an energy storage term (ε') which is ideally maximized, and an electrical loss term (ε"), i.e., the loss factor, which is ideally minimized. Likewise, the electrical losses can be expressed as the tangent of the dielectric loss angle (δ), i.e., the loss tangent. A material's loss factor (e") is the product of its loss tangent and known dielectric constant (ε_r), and therefore the loss factor (ε") and the loss tangent (tan δ) are interrelated characteristics. In most naturally-occurring materials, an increasing value for the energy storage term (ε') coincides with an increase in the value of the loss factor (ε"), thus resulting in a linked or coupled relationship. An ideal dielectric would therefore have a relatively high energy storage value accompanied by minimal electrical losses. However, in most naturally-occurring dielectrics a relatively high energy storage value typically coincides with relatively high electrical losses, which can potentially render an otherwise satisfactory dielectric less than optimal when it is used for certain purposes or applications [2].

Recently our group has developed a facile, solventless method for the decoration of multi-walled carbon nanotubes (MWCNTs) with metal nanoparticles [3, 4]. The straightforward two-step process utilizes neither reducing agents nor electric current and involves the dry mixing of a precursor metal salt (e.g. a metal acetate) with carbon nanotubes (single- or multi-walled) followed by heating in an inert atmosphere. The procedure is scalable to multi-gram quantities and generally applicable to various carbon substrates (e.g. carbon nanofiber, expanded graphite, and carbon black) and many metal salts (e.g. Ag, Au, Co, Ni, Pt and Pd acetates). There are also several wet methods available for depositing metal nanoparticles onto MWCNTs that have been discussed in [4].

The preparation and characterization of metal decorated MWCNTs has led to a significant breakthrough in the area of tailorable dielectric materials. The novel materials consist of aligned MWCNTs decorated with metal particles of nanometer dimensions distributed in a polymer matrix. It was noted that with the preferential alignment of MWCNTs in a polymer matrix and the inclusion of Ag nanoparticles, a decoupling of ε' in relation to ε" and loss tan δ occurred [5]. In addition, the disconnection between the dielectric and the loss factor were found to be

controlled by varying the amount of Ag particles that were attached to the MWCNT surface. The decoupling and independent control of these fundamental electrical material parameters offer a class of materials useful in a variety of applications in electronics, electromagnetics, and microwave engineering with potential future applications into the optical frequency regime [6-8].

These novel materials offers product designers the ability to develop new applications including new low-mass ultra-thin microstrip antennas with enhanced performance characteristics, very thin low profile substrates for Radio Frequency Identification (RFID) antennas, higher capacity low volume capacitors, High-Q dielectric resonators used in high frequency oscillators and filters, dielectric substrates for high frequency electronics, new anode/cathode materials for efficient low resistance low-loss battery components, membrane electrode assemblies, fuel cell components, components of various multifunctional material systems such as substrates for integrated sensors or solar cells, and particularly as potential materials for High-K gate dielectrics in Complementary Metal-Oxide-Semiconductor (CMOS) technology [9].

2. EXPERIMENTAL

2.1. Ag/MWCNT Synthesis and Characterization

The general procedure for preparing Ag-decorated MWCNTs involves heating a mixture of MWCNTs and Ag salt in a nitrogen oven at the decomposition temperature of the Ag salt for 3-5 hours. Details of this method have been described in a US Patent Publication [3]. Three samples were prepared – the first one where the theoretical amount of metallic Ag after decomposition of the acetate salt was 9% by weight, the second one where it was 23% by weight and the third one where it was 33% by weight. Table 1 denotes the various samples that were prepared and henceforth sample key codes will be used throughout the paper. To determine the distribution of the metal particles on the nanotubes, high resolution scanning electron microscopy (HRSEM) images were obtained using a Hitachi S-5200 field emission scanning electron microscope (FE-SEM) equipped with a through the lens (TTL) electron detector and an Energy Dispersive Spectroscopy (EDS) detector (EDAX, Mahwah, New Jersey). X-ray diffraction (XRD) analyses were performed on Siemens D5000 X-ray diffractometer or Scintag XDS-2000 Powder Diffraction System, both with Cu K_α as the radiation sources (λ = 1.5418 Å).

2.2 Materials Processing

To determine the effect of Ag/MWCNT alignments on the electric field and the electromagnetic properties, Ag/MWCNT/polymer samples were prepared as described below.

2.2.1. Parallel Alignment to flow direction

The MWCNT/Ag samples prepared as described above were melt-mixed at a loading level of 20 wt% with Ultem™ 1000 (GE Plastics) in a Brabender Plasticorder PL 2000 (30 cc capacity) at a temperature of 325 °C and 25 rpm for 3 hours. The torque values obtained during mixing in the Plasticorder were used to calculate the melt viscosities of the samples to determine if the materials can be extruded. Upon completion of mixing the material was ground in a Mini-Granulator (Kayeness, Inc) using a 5.5 mm screen and then extruded through a Laboratory Mixing Extruder (LME, Dynisco, Inc) at a barrel temperature of 170 °C and a die temperature of 350 °C. The dimensions of the die were 0.38 mm x 19.1 mm. The primary purpose of extrusion was to align the Ag-decorated MWCNTs in the direction of flow.

2.2.2. Perpendicular Alignment to flow direction

Once extruded, the ribbons were cut into pieces approximately 2 cm x 2 cm. They were then stacked on one side of a 9 cm x 2 cm x 3 cm (i.d.) mold and the remainder of the mold filled with Ultem™ 1000 pellets. The stacked ribbons were compression molded at 270 °C, 1.72 MPa, for 3 hours. The molded samples were sliced using an Isomet low speed saw with a diamond wafering blade 10.2 cm diameter and 0.3 mm thick with 15 HC diamond (Buehler Ltd).

2.3. Electromagnetic Characterization

A HP 8510C Vector Network Analyzer (VNA) was used to measure the scattering parameters of the baseline polymer material matrix and the aligned MWCNTs at microwave frequencies. Energy from the VNA was generated by an RF source and directed from the test port through an X-band (8.2-12.4 GHz) waveguide and into target sample test materials. The magnitude and phase response of the material under test (MUT) to the incident stimulus of microwave energy was measured and recorded. The observable phenomena known as scattering parameters included S_{11}, the forward reflection coefficient; S_{21}, the forward transmission coefficient; S_{22}, the reverse reflection coefficient; and S_{12}, the reverse transmission coefficient, as measured in decibels. From these quantities the dielectric properties were calculated using a data acquisition computer and the HP 85071E Materials Measurement software. The various material parameters such as the real and imaginary parts of permittivity (ε' and ε", respectively) and the loss tangent (tan δ) were plotted as a function of frequency.

2.3.1 Sample Preparation for Electronics Characterization

The MWCNT/Ag polymer ribbon samples were cut and stacked to fit a waveguide sample holder corresponding to the test frequency band of interest. The thickness of any given sample was appropriate for the selected test frequency to allow for sufficient phase discrimination by the VNA.

2.3.2 Waveguide Test Fixture

An optical breadboard test fixture and positioner with mounted waveguide apparatus was used. This fixture allows for the waveguide to be opened and closed many times in a highly repeatable manner. The port 1 side of the waveguide, along with its attached transmission line, was fixed in place. The port 2 side of the waveguide was allowed, by means of a slide positioner, to accommodate a sample and then close in precisely at the same place where it had been during the calibration sequence. The phase stable cable attached to the movable side of the waveguide was disturbed as little as possible since gross cable movements can produce measurable differences in the results.

2.3.3 Calibration

Prior to conducting material measurements, a "Full 2-Port" VNA calibration was performed. The calibration corrects for systematic measurement errors inherent to the instrument by referencing known boundary conditions [10].

2.4. Electrical and magnetoresistance measurements

Electrical resistance measurements were conducted on extruded samples of Ultem™/MWCNT/Ag composites as a function of temperature at a zero magnetic field, and as a

function of magnetic field at constant temperatures. Similar to the 4-point resistance measurement, four electrical leads were attached onto the sample surface using silver paint. Separation of the neighboring electrodes was between 1 and 2 mm, and the length of the electrodes was 5-6 mm. The studied sample was placed in the cryostat where the temperature of the sample could be varied from room temperature to 3 K and a magnetic field (H) could be applied in parallel to the sample surface. For the magnetoresistance measurement, the sample temperature was set at a pre-determined value while magnetic field scanned from 5 to -5 Teslas and from -5 to 5 Teslas. A full cycle magnetic scan provided the opportunity to check on the possible existence of hysteresis as well as the consistency of measured results. Magnetoresistance was calculated using the R(H)/R(0) - 1, where R(0) is the electrical resistance at zero magnetic field and H is the magnetic field strength. Results of the resistance measurements included those of voltages applied parallel and perpendicular to the axial direction of MWCNTs. Curves of surface resistivity of the conducting samples as a function of temperature for both directions of the applied voltages were plotted. I-V curves (current vs. voltage) were obtained by measuring the current as voltage is scanned from negative to positive values. Differential resistance/conductance can thus be calculated and plotted against applied voltage [11]. Samples for the measurements were polyimide composites loaded with bare MWCNTs, and Ag/MWCNTs. The measured samples were cut from extruded ribbons and have the typical size of 17 mm x 7 mm x 0.3 mm.

3. RESULTS AND DISCUSSION

3.1 Sample characterization

Figure 1 shows the HRSEM images of neat MWCNTs (1a) and Ag-1 samples. As evident from the images, Ag particles can be seen attached to the nanotubes. At higher magnification it was seen that these particles are between 40 and 60 nm in size. EDS was carried out on the Ag-1 samples that proved the presence of Ag particles on the MWCNTs. The samples were mounted on an aluminum stub using gold paste. Fig 1d shows the spectrum that was obtained. The Fe peak is from the catalyst in the MWCNTs and the Al and Au peaks are from the stub and the paste, respectively.

XRD investigations confirmed the 0-valence nature of the Ag nanoparticles. As shown in Figure 2, the XRD spectrum of both Ag-1 and Ag-2 exhibited the signature peaks of Ag metal at 38.0°, 44.2°, 64.3°, and 77.2°, corresponding to the (111), (200), (220), and (311) crystal planes of Ag^0, respectively. The lack of any remaining acetate diffraction patterns in the spectrum of the final mixture also suggests that the salt-to-metal conversion was essentially complete.

Figure 3 shows the HRSEM images of the Ag/MWCNTs after melt mixing with Ultem™ and extrusion of the mixture. It can be observed that the MWCNTs are predominantly oriented in the direction of extrusion (denoted by the arrow). However, the Ag particles that had been clearly visible in the neat MWCNTs are not visible now. It might be a possibility that the particles (and the nanotubes) are now coated with layers of polymer as a result of processing. In order to check the presence of Ag in the sample, EDS was carried out on the Ag-1 samples. Fig 4 shows the spectrum of the sample. As evident from the element peaks in the spectrum, there is a significant amount of Ag in the Ultem™/MWCNT sample.

3.2 Electrical resistance

Electrical resistivity of the samples was found to vary with the percentage of Ag in a quite dramatic way. The 20 wt% MWCNT (without Ag) samples had the lowest resistivity among the samples measured. At room temperature, it was in the range of 70 -200 ohm/mm^2 depending on the orientation of applied voltage to the axial direction of MWCNTs. Higher resistance was observed when the applied voltage was perpendicular to the MWCNT alignment.

The Ag-1 samples had a resistivity of 250-350 ohm/mm^2. The Ag-3 samples had a resistivity close to 1x10^5 ohm/mm^2 and exhibited the least anisotropy. The Ag-2 samples were categorized as insulators. With 20 dc Volts applied, currents in the Ag-2 samples were unstable and in the pico-ampere range. Figure 5 exhibits the curves of surface resistivity of the conducting samples as a function of temperature for both directions of the applied voltages. As observed, the resistance had a relatively pronounced increase at low temperatures for all the samples. The increases were slightly larger when voltages were applied in the parallel direction. The Ag-1 samples have higher resistance than the 20 wt% MWCNT composites. The higher resistance was most likely due to the less loading of MWCNTs in the Ag/MWCNT-Ultem™ mixture. The 9 wt% Ag could not sufficiently compensate for the loss of current conduction because of a lesser amount of CNTs, however, it seemed to improve the conduction between CNTs, as it was revealed by the decrease in anisotropy of resistivity. Furthermore, resistance data of the 20 wt% MWCNT and Ag-1 samples could be fitted with the curves of Exp(C/T) (where C is a MWCNT loading dependent constant) from room temperature to 5 K, and that of the Ag-3 samples from 200 K to 5 K. The exponential proportion to 1/T could be an indication of currents being conducted via a tunneling mechanism. Figure 6 shows the temperature dependent variations of currents for the same set of samples. For comparison, the currents were normalized to their respective magnitude at 100 K. It could be observed that, instead of increasing with temperature as those of 20% MWCNT and Ag-1 composites, currents in the samples of Ag-3 composites decreased with increasing temperature at temperatures above 200 K, for both orientations of the applied voltages. The decrease in current with increasing temperature was a metal-like behavior and implied that, at high temperatures, substantial portion of currents were conducted through the Ag components in the composites and it was also indicated by the data of differential conductance. However, at low temperatures, conduction through CNTs and tunneling through the contacts of CNTs were the predominant mechanisms for transporting the electrons.

Regarding the insulation of Ag-2, it may be that the 23 wt% of Ag had a large enough mass to enhance potential barriers for preventing electrons from tunneling between CNTs, but it was under the threshold for electrons to find a conduction network for percolating.

3.3 Magnetoresistance

Figure 7 displays the magnetoresistance as a function of magnetic field at temperatures of 3, 5, 10, 20, 50, 100, and 200 K for the composite sample of 20 wt% MWCNT in Ultem™. Voltage was applied in the direction perpendicular to the axial direction of the MWCNTs. As seen from the figure, the magnetoresistance of the composite was negative and decreased monotonically with the increasing magnitude of magnetic field. Also, the magnetoresistance was enhanced in magnitude at low temperatures. No magnetic hysteresis was observed and Figure 7 exhibits the typical magnetoresistance behavior of MWCNT-polymer composites, including conducting samples loaded with MWCNT/Ag. Different weight percentages of Ag on the MWCNTs

affected the magnetoresistance quantitatively. For samples with same loading of MWCNTs, voltage applied in perpendicular direction had a larger response to the applied magnetic field as compared with those in the parallel direction.

I-V curves (current vs. voltage) were obtained by measuring the current when the voltage was scanned from negative to positive values. Differential resistance/conductance could thus be calculated and plotted against the applied voltage. For the samples of 20 wt% MWCNT and Ag-1 composites, differential conductance increased with voltages at temperatures lower than 100 K and remained constant at temperatures 100 K and above. For the Ag-3 composites, the differential conductance increased with voltages at all temperatures and showed slope changes at higher voltages. Figure 8 compares the normalized differential conductance of the Ag-1 samples when voltage was applied in parallel to the MWCNTs at a temperature of 3 K with those when the voltage applied was in the perpendicular direction. The differential conductance (dI/dV) was normalized to its value at 0 voltages. A dip on the curve at low voltages ($|V| < 0.2V$) was considered as a suppression of conductance and was even more pronounced for the perpendicular direction. The dip was attributed to the strong electron-electron (e-e) interaction in and between the MWCNTs. With the strong e-e interaction, a coulomb gap may be opened and electron motion was via the hopping mechanism. These dips did not show up at high temperatures for both directions. The suppression of conductance was also observed for the 20 wt% MWCNT composites but not for the Ag-3 composites.

As mentioned previously, there was enough Ag in the Ag-3 samples to provide additional paths for the electron transport. The differential conductance of the Ag-3 samples displayed in Figure 9 had slope changes for both directions of the applied voltages. The changes in slope may be an indication of the change in preferred current paths. As observed at low voltages, the currents were mainly conducting through the MWCNTs, as those in the samples of 20 wt% MWCNTs and Ag-1 composites. At higher voltages, the currents had more conducting paths through the silver. The slope change of differential conductance vs. voltage was observed at temperatures up to 300 K.

3.4 Electromagnetic Properties

The materials used for testing comprise of extruded samples of MWCNTs, decorated with and without Ag particles, dispersed in an Ultem 1000™ matrix and have a preferential or predetermined alignment with respect to an orientation of an electrical field that is incident to the length-wise axis or orientation of the tubes. This predetermined alignment of the network can be horizontal, vertical or longitudinal.

In the horizontal alignment, [Figure 10(a)], the CNTs were horizontally aligned with respect to the orientation of the electrical field (arrow E). Incidental energy (propagating in the direction k) entered the dielectric through the first port (Port 1), with some portion of the incident energy (flowing in the direction k) being reflected as represented by the arrow R. Transmitted energy (arrow T) exited the dielectric through a second port (Port 2). Energy was also attenuated (A not shown) within the material, thus reducing the magnitude and altering the phase of the transmitted energy. By means of a law of conservation the reflected energy (R) + transmitted energy (T) + attenuated energy (A) must equal the total energy. From this conservation relationship the electrical dissipation or loss within the dielectric was determined [12, 13]. The values reported

were the data obtained at 10 GHz. As seen from Figure 10(b), the magnitude of the energy storage term (ε') was at an observed minimum in the neat polymer. As the loading level of CNTs was increased to 5 wt%, the magnitude of ε' more than doubled, increasing yet again by approximately 50% as the loading percentage increased to 10 wt%. At 20 wt% loading of the CNTs, the magnitude of ε' increased to a peak magnitude with a very rapid increase of permittivity between these two loading levels. However, this potentially desirable increase in ε' came with a tradeoff in the form of substantially higher losses in the dielectric. At this loading level, the metalized samples were tested. The magnitude of ε' was clearly reduced by the presence of the Ag nanoparticles. However, for the Ag-1 samples, the magnitude of ε' remained relatively high compared to the 0, 5, and 10 wt% samples. For Ag-2 samples, the magnitude of ε' was approximately equal to that of the 5 wt% MWCNTs. A similar pattern was observed in case of the loss factor (ε") that was clearly reduced by the introduction of the Ag nanoparticles. In Ag-1, ε" was reduced by approximately 75%, with an approximate 30% reduction in the magnitude of the ε'. For Ag-2 ε" was effectively reduced to zero. Therefore, by varying the loading percentages of the Ag in the MWCNTs, the loss factor was minimized without unduly minimizing the value of the energy storage term. The magnitude of the loss tangent (tan δ) was also plotted against the material loading % and the values increased sharply when the loading level of MWCNTs was increased from 10 to 20 wt%. Upon addition of Ag into a horizontally-aligned network, the magnitude of the loss tangent was reduced by approximately 70% in Ag-1 samples. For Ag-2, tan δ was effectively reduced to zero, albeit with some additional but minimal reduction in the magnitude of ε'.

Figure 11(a) denotes a similar experimental set-up as Figure 10 (a) with the exception of the orientation of the MWCNT network being generally vertical. As with Figure 10 (b), Figure 11 (b) shows that the magnitude of ε' increased or spiked dramatically as the loading percentage of the CNTs increased from 10 to 20 wt%. For Ag-1, this magnitude decreased somewhat but remained substantially higher than that exhibited during horizontal alignment. Additional loading of Ag (Ag-2) was observed to have a negligible effect on the magnitude of the energy storage value. ε" increased dramatically when the loading of MWCNTs was increased from 10 to 20 wt%. However, ε" was substantially reduced with the introduction of Ag in Ag-1. In the exemplary data of Figure 11(b), an approximately 90% reduction in the value of ε" was observed which corresponded to a substantially lower reduction in the magnitude of the ε'. Likewise, an approximately 90% reduction in the loss tangent was observed between a peak value at 20 wt% MWCNT loading and Ag-1. Additional Ag loading had a negligible effect on ε" and tan δ.

Based on the data shown in Figures 10 and 11, it can be concluded that the MWCNT/Ag samples demonstrate a unique ability to "decouple" the energy storage term or value, i.e., the ε' factor, of a given material's electrical permittivity from the materials' electrical loss term or ε" factor when oriented or aligned in a preferential or predetermined manner. The ε' and ε" of these materials could be effectively decoupled from each other and independently controlled or modified by varying the preferred alignment of the network and/or the loading percentage of the nanoparticles, and/or by varying the size and/or distribution of the metal-based nanoparticles so as to enable a class of engineered dielectric materials that could be useful in a host of applications [14, 15]. Such applications can include, but are not limited to, a potential material for use in Complementary Metal-Oxide-Semiconductor (CMOS) technology, microwave engineering applications, RF communications and controls, optics, etc.

Figure 12 describes a different set of exemplary observed electrical phenomena in the aligned network i.e., the scatter parameters or S-Parameters. The S-parameters describe the transmission and reflection of high-frequency traveling waves within a transmission line in the form of reflection and transmission coefficients. The magnitudes of each of the reflection coefficients and transmission coefficients of the network were plotted against the material loading percentages. In the case of horizontal alignment [Figure 12(a)], increased MWCNT loading levels in the polymer matrix generally reduced the transmission coefficient while increasing the reflection coefficient, a potentially undesirable tradeoff. The crossover point at around 15 wt% indicates the point where the network connectivity achieves prominence. However, with the addition of the Ag nanoparticles, both the transmission coefficient and the reflection coefficient remained relatively unchanged. That is, the potential performance benefits provided by the introduction of the Ag nanoparticles were not themselves adversely affected by a corresponding degradation in the S-parameters, which is itself a useful characteristic**.** For the vertical alignment [Figure 12(b)], increased MWCNT loading levels beyond 5% generally reduced the transmission coefficient while in this instance also reduced the reflection coefficient. However, with the addition of Ag nanoparticles, the transmission coefficient showed an upward trend, while the reflection coefficient showed a downward trend, again a potentially useful electrical phenomenon. Immediately beyond a silver loading level of 9 wt%, a crossover occurs and the reflection coefficient decreases indicating a decrease in electrical conductivity of the system. This data is synchronous with the observations in section 3.2 where the Ag-2 samples became insulators.

4. SUMMARY

A novel and solventless method was used to deposit Ag nanoparticles on MWCNTs. These were then compounded with a polyimide and extruded in order to preferentially align the CNTs. Extruded samples were subjected to a variety of electromagnetic experiments. Electrical resistivity of the samples was found to vary with the percentage of Ag in a quite dramatic way. It was observed that the currents increased with temperature in the MWCNT loaded composites as well as the Ag-1 composites. However, currents in the samples of Ag-3 composites decreased with increasing temperature at temperatures above 200 K, for both orientations of the applied voltages. The decrease in current with increasing temperature was a metal-like behavior and implied that, at high temperatures, substantial portion of currents were conducted through the Ag components in the composites. The data also showed differential conductance at low temperatures indicating that the conduction was through the CNTs via contacts and a tunneling mechanism. Similarly, at low voltages, the currents were mainly conducting through the MWCNTs, as those in the samples of 20 wt% MWCNTs and Ag-1 composites whereas, at higher voltages, the currents had more conducting paths through the silver.

For the measurement of electromagnetic properties, the network of MWCNTs (with or without Ag) was preferentially aligned with respect to an incident electrical field. For Ag-1 and Ag-2 samples, the electrical permittivity, ε', of the dielectric was effectively decoupled from its electrical loss, ε". This decoupling effect of the energy storage value from the electrical loss value is tailorable by varying the preferred alignment of the network and/or the loading percentage of the nanoparticles, and/or by varying the size and/or distribution of the metal-based nanoparticles. This opens up a pathway to generate a class of engineered dielectric materials that

could be useful in a host of applications such as a potential material for use in Complementary Metal-Oxide-Semiconductor (CMOS) technology, microwave engineering applications, RF communications and controls and optics. Future studies are warranted relating the electrical resistivity data to the decoupling of dielectric properties.

Acknowledgements

The authors wish to acknowledge the help received from Dennis C. Working of NASA LaRC. They would also like to thank Dr. Peter T. Lillehei of NASA LaRC for his valuable comments.

5. Figures & Tables

Table 1

Sample name	Sample details
Ag-1	9 wt% Ag attached to MWCNTs; 20 wt% of the mixture added to Ultem™. So in the polymer matrix, filler is theoretically 18.2 wt% MWCNT and 1.8 wt% Ag.
Ag-2	23 wt% Ag attached to MWCNTs; 20 wt% of the mixture added to Ultem™. So in the polymer matrix, filler is theoretically 15.4 wt% MWCNT and 4.6 wt% Ag.
Ag-3	33 wt% Ag attached to MWCNTs; 20 wt% of the mixture added to Ultem™. So in the polymer matrix, filler is theoretically 13.3 wt% MWCNT and 6.7 wt% Ag.

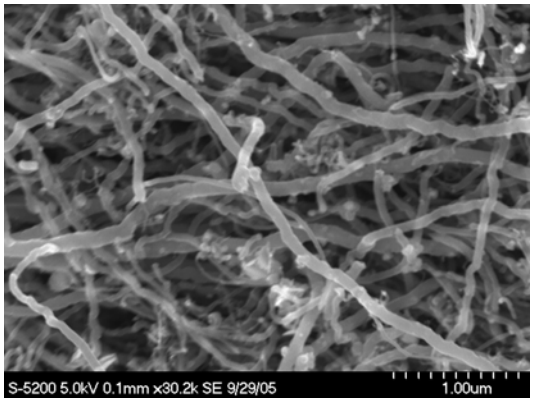

(a) neat MWCNTs

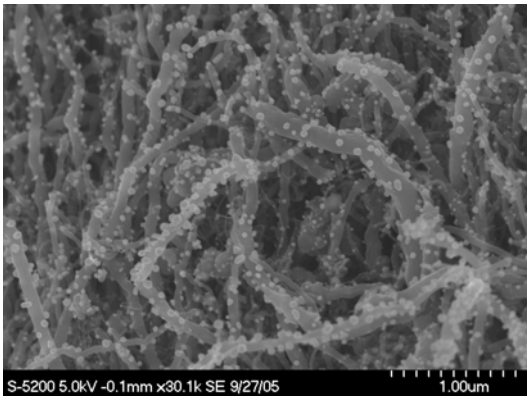

(b) Ag-1

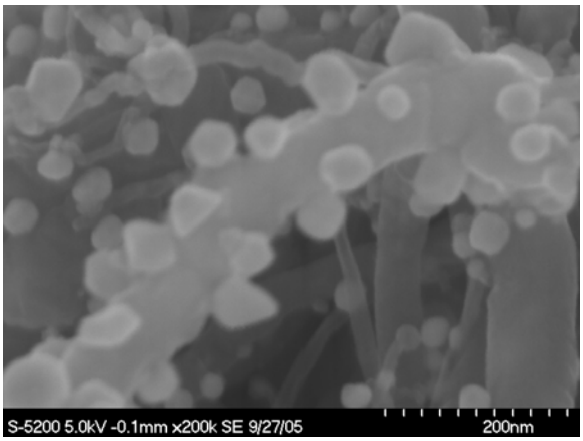

(c) Ag-10

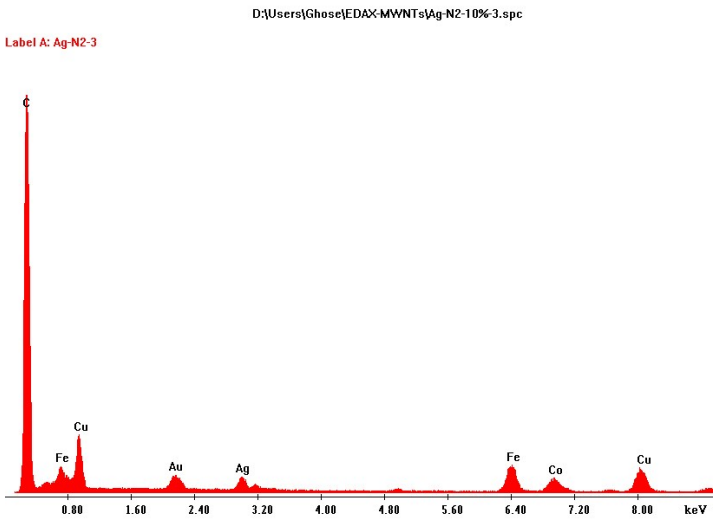

Figure 1: HRSEM of MWCNTs with (a) neat, (b) Ag-1, (c) Ag-2 (higher magnification) (d) EDAX on sample

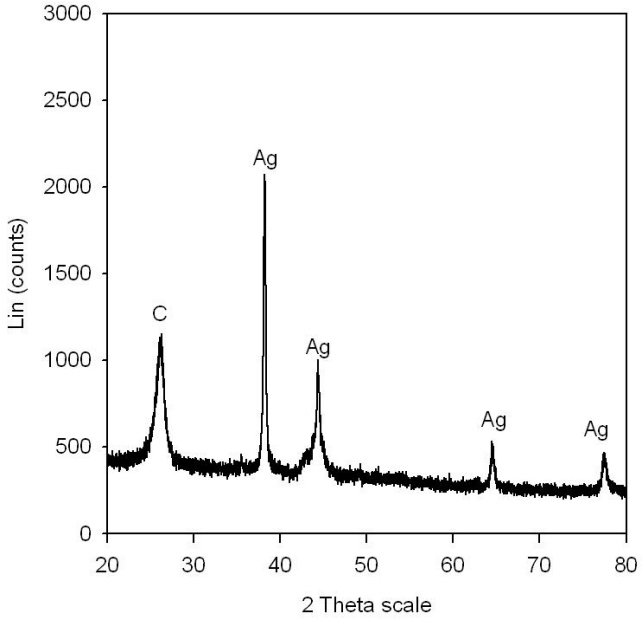

Figure 2(a)

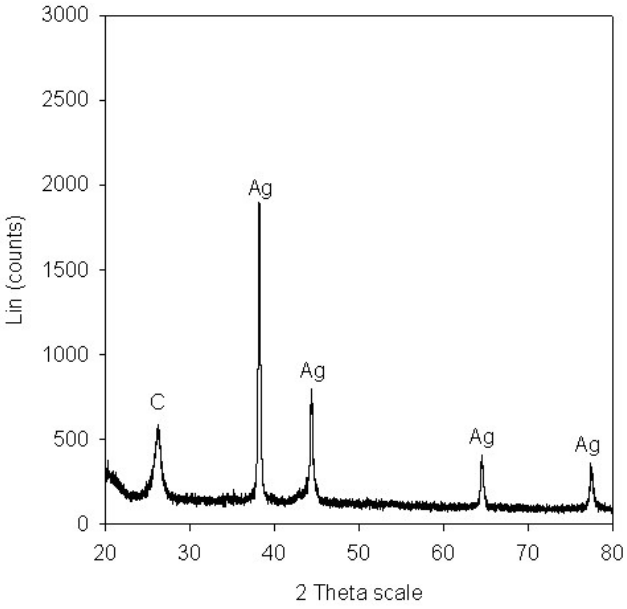

Figure 2(b)

Figure 2: XRD patterns of MWCNT/Ag mixtures of (a) Ag-1 and (b) Ag-2

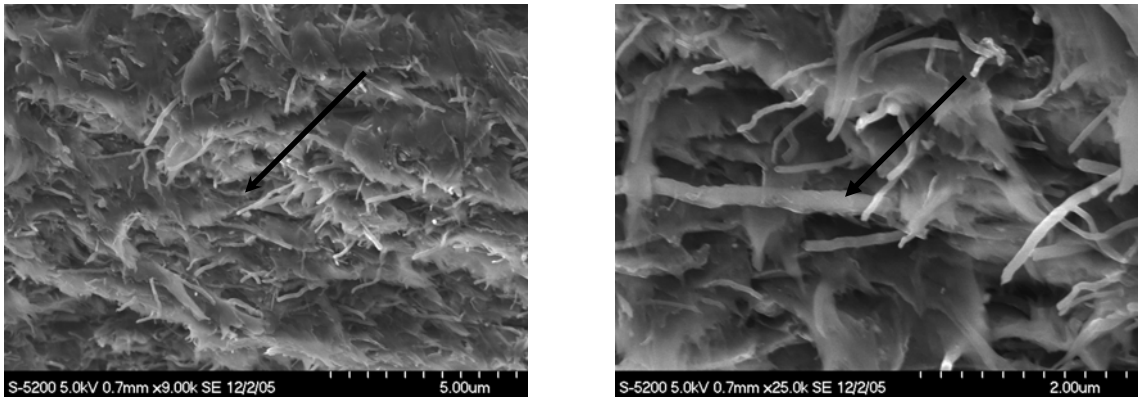

Figure 3: HRSEM of Ag-1; arrow denotes flow direction

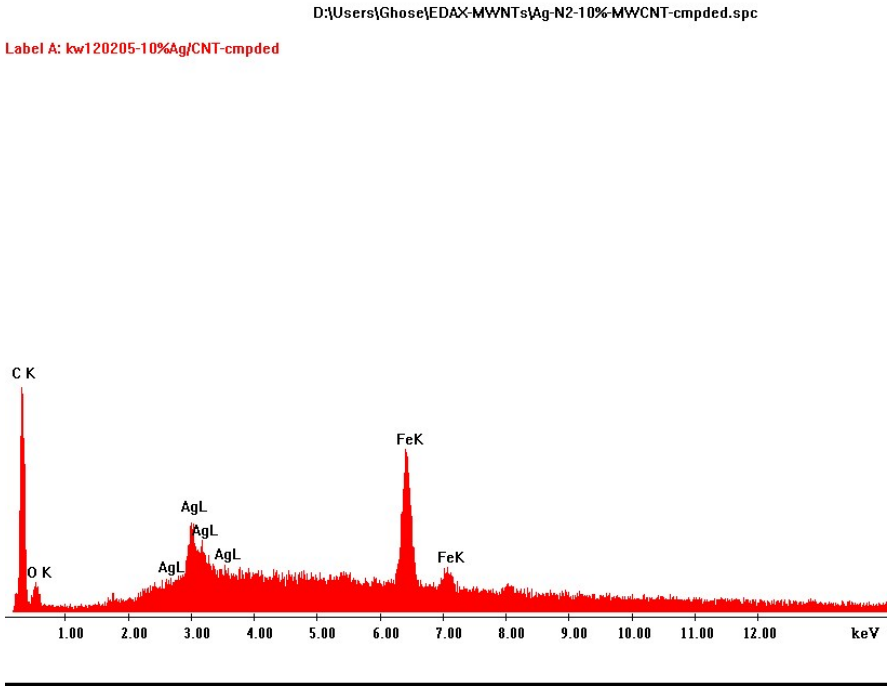

Figure 4: EDS on Ag-1

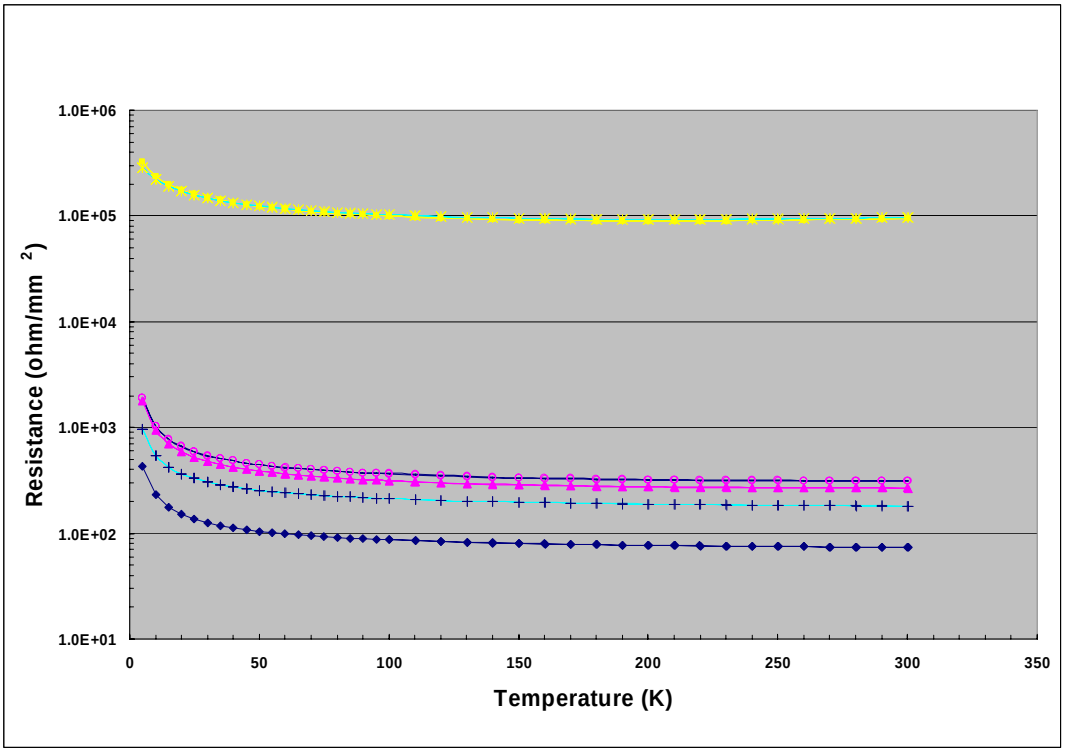

Figure 5: Temperature dependent electrical resistivity of MWCNTs-loaded Ultem™ composites. Curves from bottom to top are for the resistivity of 20 wt% MWCNT sample when voltage applied in parallel to the axial direction of CNTs(♦), in perpendicular to the CNTs (+), Ag-1 when voltage in parallel (▲), in perpendicular (o), Ag-3 when voltage in parallel (■), and in perpendicular(*) respectively. Resistivity increased for all samples at low temperatures.

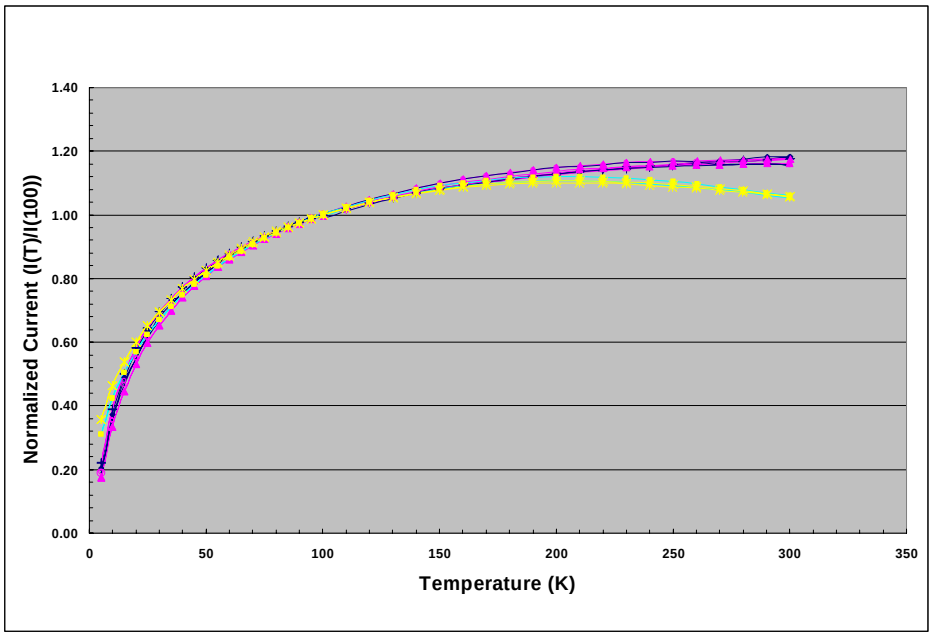

Figure 6: Normalized currents as a function of temperature for the samples of 20 wt% MWCNT (curves with ♦, and + respectively), Ag-1 (▲ and O respectively), and Ag-3 (■ and * respectively) composites. Currents in Ag-3 samples decreased with increasing temperature at temperatures above 200 K.

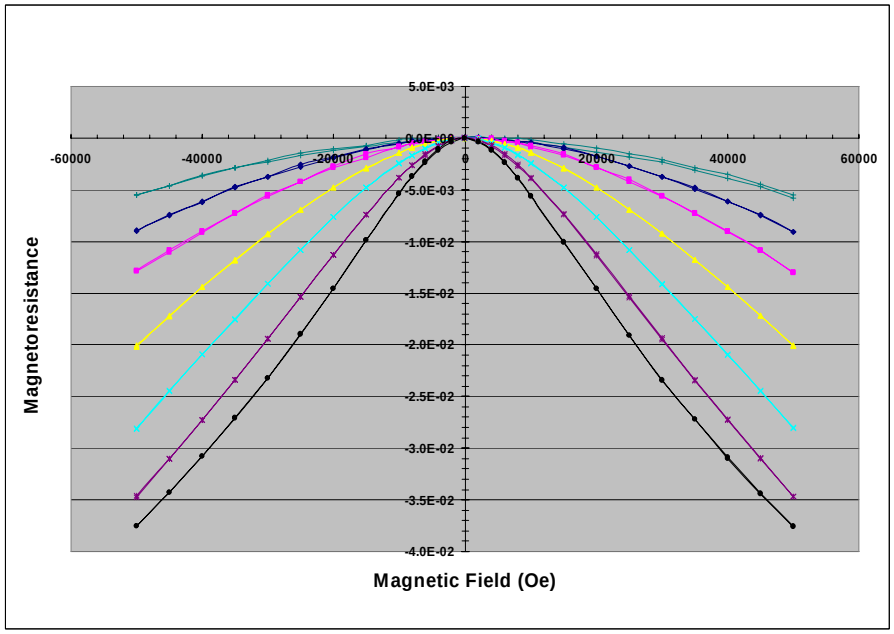

Figure 7: Magnetoresistance at various temperatures for the 20 wt% MWCNT-Ultem™ thick film sample. Curves shown from bottom to top are the magnetoresistance at 3, 5, 10, 20, 50, 100, and 200 K respectively. Voltage was applied perpendicular to the CNT axial direction.

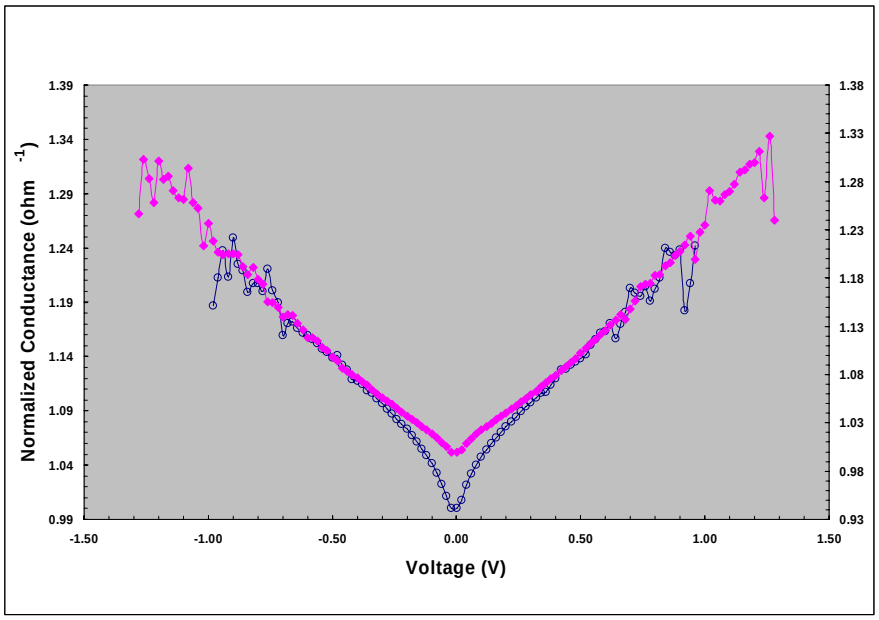

Figure 8: Comparison of normalized differential conductance of Ag-1 samples for both directions of the applied voltage at 3K. Curve with ♦ is for the parallel direction and use the y-scale on the right side of figure, and that with O is for the perpendicular direction and use the y-scale on the left.

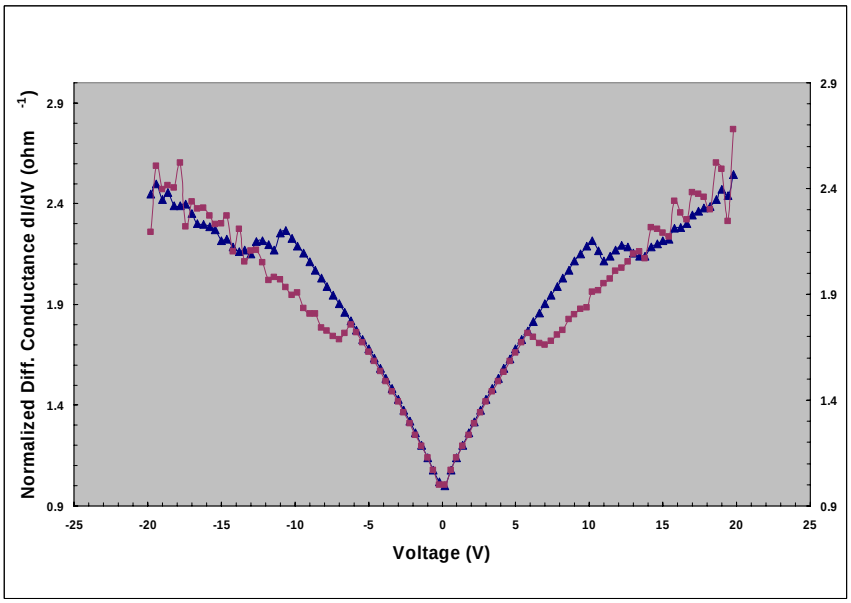

Figure 9: Normalized differential conductance of Ag-3 samples for both directions of the applied voltage at 10 K. Curve with ▲ is for the parallel direction and use the y-scale on the left side of the figure, and that with ■ is for the perpendicular direction and use the y-axis on the right. At low voltages, the currents conducted mainly through the MWCNTs. At high voltages, the currents preferred to go through the Ag components in the composites.

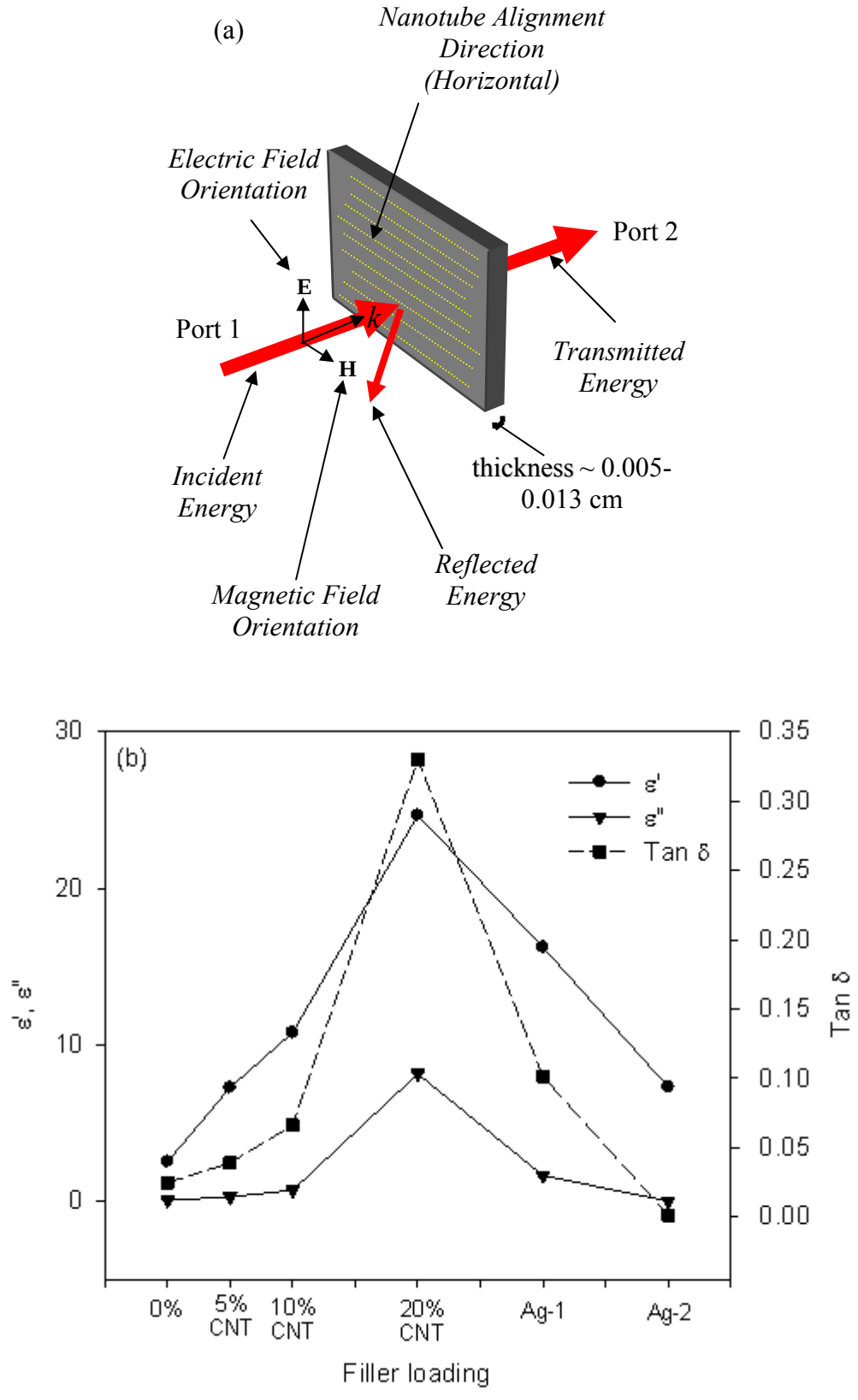

Figure 10: Permittivity, loss and loss tangent of horizontally aligned MWCNT samples

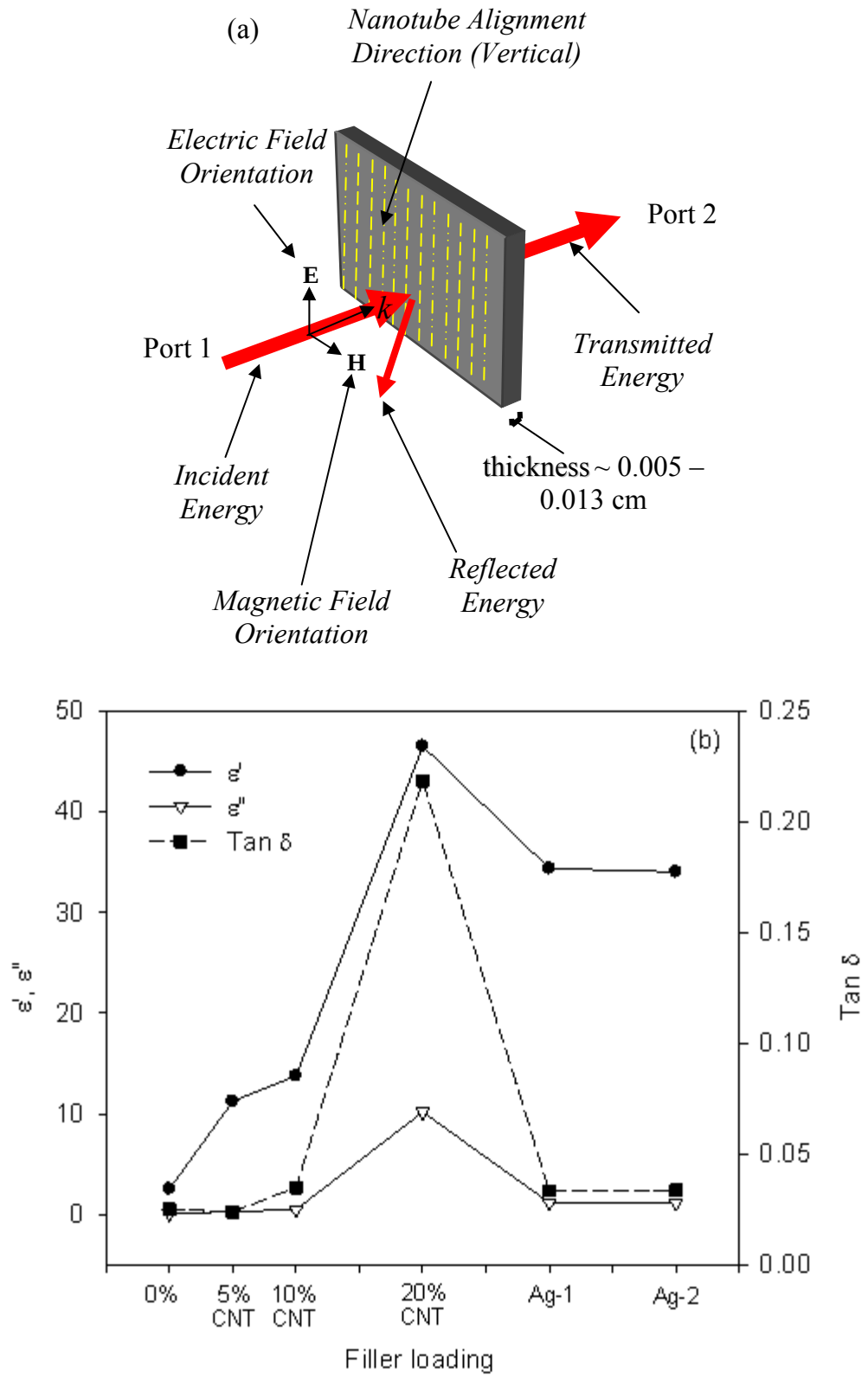

Figure 11: Permittivity, loss and loss tangent of vertically aligned MWCNT samples

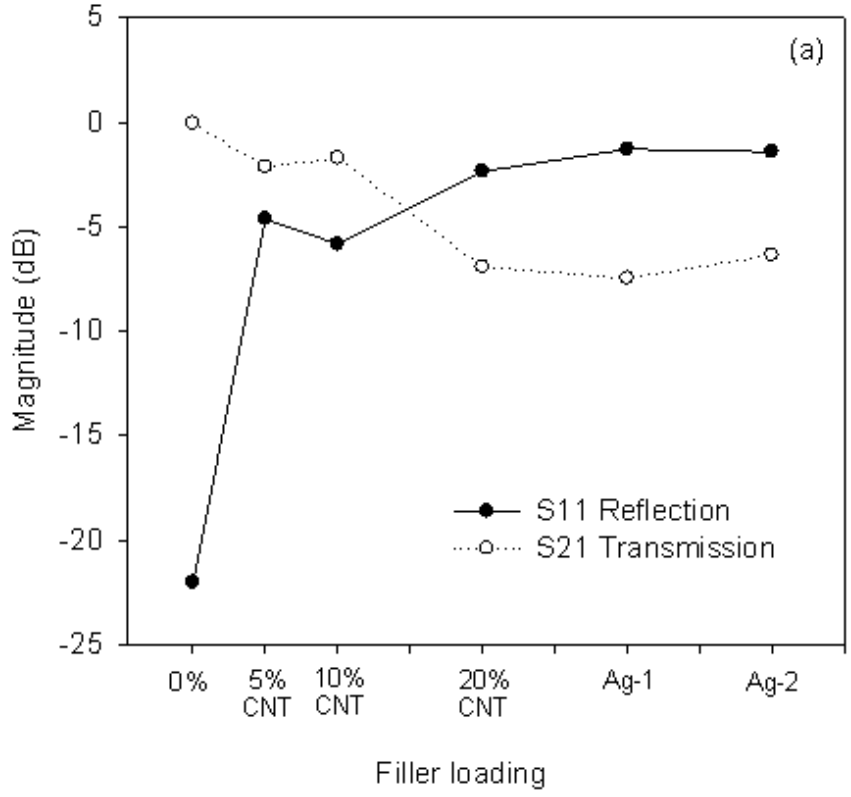
(a)
5
0
-5
-10
-15
-20
-25
Magnitude (dB)
S11 Reflection
S21 Transmission
0%
5% CNT
10% CNT
20% CNT
Ag-1
Ag-2
Filler loading

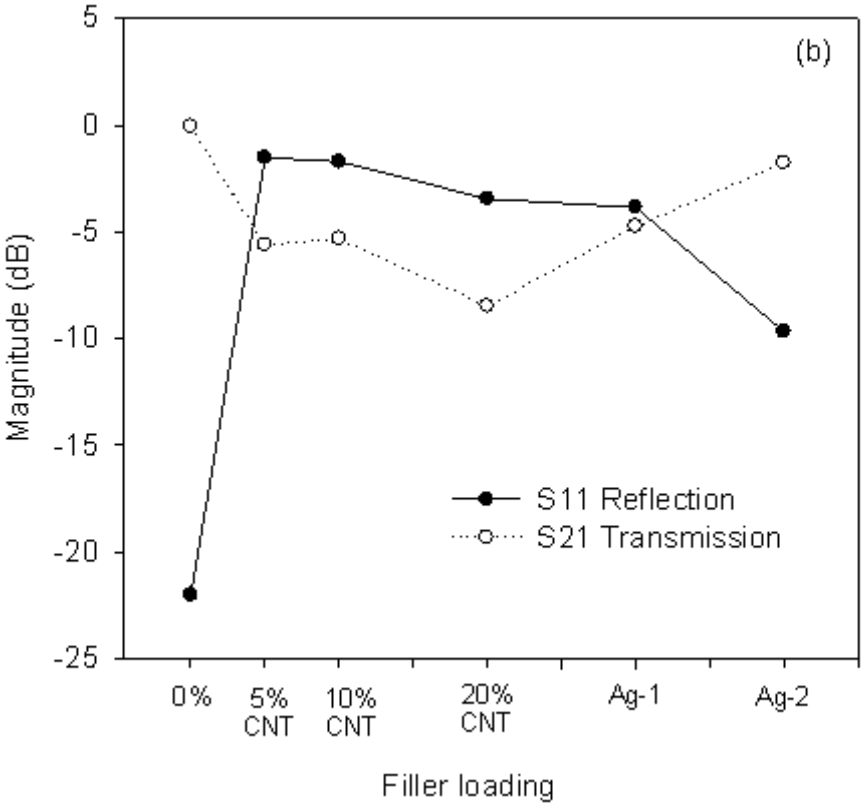
(b)
5
0
-5
-10
-15
-20
-25
Magnitude (dB)
S11 Reflection
S21 Transmission
0%
5% CNT
10% CNT
20% CNT
Ag-1
Ag-2
Filler loading

Figure 12: S-parameters in horizontal alignment (a) and vertical alignment (b)

6. References

1. A. R. Von Hipple, “Dielectrics and Waves”, John-Wiley, 1954.

2. A. R. Von Hipple, "Dielectric Materials and Applications", MIT Press, 1954.

3. United States Patent Application No. 20070292699, “Method of Depositing Metals onto Carbon Allotropes and Compositions Therefrom”, December 20th 2007. WIPO Pub No.: WO/2008/048349, Pub date April 24th 2008.

4. Yi Lin, Kent A. Watson, Michael J. Fallbach, Sayata Ghose, Joseph G. Smith, Jr., Donavon M. Delozier, Wei Cao, Roy E. Crooks, and John W. Connell, “Facile, Solventless Preparation and Characterization of Metal Nanoparticle-Decorated Carbon Nanotubes”, submitted to ACS Nano (January 2009).

5. United States Patent Application No. 20090022977, "Tailorable Dielectric Materials with Complex Permittivity Characteristics providing High Dielectric Constants and Low Loss Factors” January 22, 2009.

6. Charles P. Poole Jr. and Frank J. Owens, “Introduction to Nanotechnology,” John Wiley and Sons, Inc. Hoboken, New Jersey, 2003.

7. Dentcho A. Genov, Andrey K. Sarychev, Vladimar M. Shalaev and Alexander Wei, "Resonant Field Enhancements from Metal Nanoparticle Arrays", Nano Letters, 2004, Vol. 4 (1), 153.

8. Ildar R. Gbitov, Robert A. Indik, Natalia M. Litchinitser, Andrei I. Maimistov, Vladimir M. Shalaev and Joshua E. Soneson, "Double-Resonant optical materials with embedded metal nanostructures." J. Opt. Soc. Am. B, 2006, Vol. 23 (3), 535.

9. Ben G. Streetman and Sanjay Banerjee, “Solid State Electronic Devices” (Fifth Edition) Prentice Hall Series in Solid State Physical Electronics, Prentice Hall, Upper Saddle River, New Jersey, 2000.

10. J. Baker-Jarvis, E. Vanzura and W. Kissick, “Improved technique for determining complex permittivity with the transmission/reflection method.” IEEE Transactions on Microwave Theory and Techniques, August 1990, Vol 38, 1096.

11. Neelakanta S. Perambur, “Handbook of Electromagnetic Materials, Monolithic and Composite Versions and Their Applications” CRC Press, Boca Raton, New York, London, Tokyo, 1995.

12. Y.L. Yang, M.C. Gupta, K.L. Dudley and R.W. Lawrence, “A comparative study of EMI shielding properties of carbon nanofiber and multiwalled carbon nanotube filled polymer composites”, Journal of Nanoscience & Nanotechnology, 2005, 5(6), 927

13. Y.L. Yang, M.C. Gupta, K.L. Dudley and R.W. Lawrence, “Conductive carbon nanofiber-polymer foam structures”, Advanced Materials, 2005, 17(16), 1999.

14. K. Chin, A. Gobel, W. Chen, H. Elim, W. Ji, G. Chong, C. Sow and A. Wee, “Gold and Silver Coated Carbon Nanotubes: An Improved Broad-Band Optical Limiter”, Chem. Phys. Lett., 2005, 409, 85.

15. B. Xue, P. Chen, Q. Hong, J. Lin and K. Tan, “Growth of Pd, Pt, Ag and Au Nanoparticles on Carbon Nanotubes”, J. Mater. Chem., 2001, 11, 2378.